

QUANTITATIVE FINANCE
RESEARCH CENTRE



UNIVERSITY OF
TECHNOLOGY SYDNEY



QUANTITATIVE FINANCE RESEARCH CENTRE

Research Paper 250

June 2009

Empirical Behavior of a World Stock Index from Intra-Day to Monthly Time Scales

Wolfgang Breymann, David Lüthi and Eckhard Platen

ISSN 1441-8010

www.qfrc.uts.edu.au

Empirical Behavior of a World Stock Index from Intra-Day to Monthly Time Scales

Wolfgang Breymann¹, David Lüthi¹ and Eckhard Platen²

June 15, 2009

Abstract

Most of the papers that study the distributional and fractal properties of financial instruments focus on stock prices or foreign exchange rates. This typically leads to mixed results concerning the distributions of log-returns and some multi-fractal properties of exchange rates, stock prices, and regional indices. This paper uses a well diversified world stock index as the central object of analysis. Such index approximates the growth optimal portfolio, which is demonstrated under the benchmark approach, it is the ideal reference unit for studying basic securities. When denominating this world index in units of a given currency, one measures the movements of the currency against the entire market. This provides a least disturbed observation of the currency dynamics. In this manner, one can expect to disentangle, e.g., the superposition of the two currencies involved in an exchange rate. This benchmark approach to the empirical analysis of financial data allows us to establish remarkable stylized facts. Most important is the observation that the repeatedly documented multi-fractal appearance of financial time series is very weak and much less pronounced than the deviation of the mono-scaling properties from Brownian-motion type scaling. The generalized Hurst exponent $H(2)$ assumes typical values between 0.55 and 0.6. Accordingly, autocorrelations of log-returns decay according to a power law, and the quadratic variation vanishes when going to vanishing observation time step size. Furthermore, one can identify the Student t distribution as the log-return distribution of a well-diversified world stock index for long time horizons when a long enough data series is used for estimation. The study of dependence properties, finally, reveals that jumps at daily horizon originate primarily in the stock market while at 5 min horizon they originate in the foreign exchange market. These results are contrasted with the behavior of foreign exchange rates. The principal message of the empirical analysis is that there is evidence that a diffusion model without multi-scaling could reasonably well model the dynamics of a broadly diversified world stock index.

¹Zurich University of Applied Science

²University of Technology, Sydney, School of Finance & Economics and Department of Mathematical Sciences, PO Box 123, Broadway, NSW, 2007, Australia

1 Introduction

1.1 Scaling Behavior and Fractal Properties

Fractal properties in financial time series, resulting in anomalous scaling, have been observed already forty years ago, Mandelbrot (1963). This picture has been confirmed and refined since 1990, Müller et al. (1990), mainly due to the availability of intra-day data. Among the empirical stylized facts discovered are volatility clustering Dacorogna et al. (2001), heavy tails of return distributions with tail indices between 3 and 5 Dacorogna et al. (2001), anomalous scaling Dacorogna et al. (2001), and multi-fractal properties Ghashghaie et al. (1996), Muzy, Delour & Bacry (2000), Breymann, Ghashghaie & Talkner (2000), Mandelbrot (2001a, 2001b, 2001c, 2001d).

There have been a large number of studies with results that are mixed or even contradicting. One thread of research presents evidence for multifractal properties, including an analogy with turbulence Ghashghaie et al. (1996) and the multifractal models of Mandelbrot (2001a, 2001b, 2001c, 2001d). The characteristic empirical properties frequently discussed are the following:

- The absolute moments of log returns $r_\Delta(t) \equiv \log P(t) - \log P(t - \Delta)$ of a price series $P(t)$ display the scaling behavior

$$E[|r_\Delta(t)|^q] \propto \Delta^{f(q)} \quad (1)$$

where $f(q) \equiv qH(q)$ is a concave function, $H(q)$ being the generalized Hurst exponent, and Δ is the time horizon of the return. If a horizon of 1 step is chosen, the time horizon is identical with the observation time step size. Such scaling behavior reflects the essence of multifractal properties

- The distributions of log returns display heavy tails at short time horizons and change their form with increasing time horizon, successively approaching the normal distribution.

Such properties have been observed for both foreign exchange rates and stock indices, see e.g. the broad studies Matteo, Aste & Dacorogna (2003, 2005), Matteo (2007) and references therein.

The models contain a kind of hierarchical structure for the volatility, which can be modeled, e.g., through a cascade structure Muzy, Delour & Bacry (2000), Bacry, Delour & Muzy (2001) or a multi-fractal time scale Calvet & Fisher (2001, 2002). If modeling is done assuming a risk-neutral martingale measure in a diffusion setting, then the familiar machinery of risk-neutral valuation of contingent claims can be used. This requires the scaling exponent of the 2nd moment to be one, $f(2) = 1$, or, equivalently, $H(2) = 0.5$.

A second thread of papers present evidence for fractional properties, which are characterized by mono-scaling behavior of the moments of absolute log returns with a linear function $f(q)$ of the form

$$f(q) = Hq \quad (2)$$

with Hurst exponent $H \neq 0.5$ being independent of q . This implies that the distribution of log returns does not change its form with increasing time horizons.

For the value of H , most authors find $H > 1/2$, which signifies the existence of trends on any time scale. Mantegna and Stanley observed abnormal scaling without multi-scaling (fractional behavior) for stock market indices Mantegna & Stanley (1995, 1997). More recently, their findings have been confirmed by other authors for regional stock indices Struzik & Kiyono (2006), Bartolozzi, Leinweber & Thomas (2005).

In our opinion the reason for the above mixed picture is that up to now the right object has not yet been studied. Typically, foreign exchange (FX) rates, stock prices or regional stock index data are analyzed. Even though these time series seem to behave roughly similarly, there are noteworthy differences. FX rates are symmetric in the sense that there should not be any structural difference in the statistical properties between the EUR/USD and the USD/EUR exchange rate. For stock indices, on the other hand, a crash is more likely than a sudden upwards price jump of the same size, so that one expects an asymmetric distribution. We will show further differences within this paper.

Then the question arises of what is the best object to study to obtain the best, which means most undistorted, information about a security like a currency. We argue that the best object of study is a broadly-diversified world stock index because it contains the important parts of the world market's systemic or general risk dynamics. Such an index has been constructed in Breymann, Kelly & Platen (2006). A widely-available index, the MSCI-world accumulation index could also be used, see Le & Platen (2006).

We would like to draw attention to the fact that such an object behaves differently under various aspects. In particular, there is no transition of the form of the return distribution to a normal distribution when the time horizon is increased; this is in contrast to common beliefs which, at least implicitly, is present in many studies on multi-fractal properties of foreign exchange or stock market data.

The outline of this paper is as followed. Section 2 describes the data and the construction of the index. In Section 3 the results are presented. The first subsection discusses the scaling behavior, the second the behavior of the autocorrelation function, the third the quadratic variation, the fourth the change of the shape of the return distributions with increasing time horizon, and the last the dependence behavior on the basis of bivariate return distributions. Section 4 concludes.

2 The Data

We study a world stock index (WSI) denominated in US dollar (USD) and eight other major currencies, as well as the foreign exchange (FX) rates of these non-dollar currencies against USD. For both, the WSI and the FX rates intra-day and daily time series are investigated.

The intra-day samples reach from 1 April 1996 to 30 June 2001. The intra-day WSI $I^{(WSI)}(t)$, which is described in detail in Breymann, Kelly & Platen (2006), is based on 34 country indices and the corresponding FX data. Denominated in

USD it is given as

$$I_{\text{USD}}^{(\text{WSI})} = \sum_{j=1}^d \delta^{(j)}(t) I_{\text{USD}}^j(t) = \sum_{j=1}^d \delta^{(j)}(t) I_i^j(t) X_{\text{USD}}^i(t). \quad (3)$$

Here, $I_i^j(t)$ denotes the j th local accumulation index denominated in currency i and held in the WSI at time t , $I_{\text{USD}}^j(t)$ denotes the same index denominated in USD, $X_{\text{USD}}^i(t)$ is the spot price of one unit of currency i when measured in USD and $\delta^{(j)}(t)$ denotes the number of units of the j th local accumulation index. The values of $\delta^{(j)}(t)$ are adjusted yearly such that they are roughly proportional to the market capitalization of the corresponding local index. The intra-day data have originally been provided by Olsen Data, who collected and cleaned them. The tick data have been regularized to 5 min data with previous-tick interpolation. Since intra-day data contain strong intra-day seasonalities of the volatility, de-seasonalization was required before further analyses. We used a transformation onto an activity-based time scale, as described in Breymann (2000) and Breymann, Dias & Embrechts (2003). In this transformation, weekends and public holidays have properly been taken into account. The procedure is available as S-Plus package Breymann (2002).

The daily samples reach from 1 Jan 1973 to 10 Mar 2006. The WSI has been constructed out of 27 local indices obtained from Thomson Financial by a procedure similar to the one used for intra-day data. The number of local indices is somewhat less than for the intra-day sample because there were less indices available that date back to 1973. Weekends and worldwide public holidays have been excluded from the sample.

The FX samples studied consist of the widely available FX data also used for the construction of the WSI samples. Notice that the FX rate of a currency j expressed in units of a currency k can be reconstructed from the WSI $I(t)$ when it is simply expressed in these two currencies:

$$X_k^j(t) = \frac{I_k(t)}{I_j(t)}. \quad (4)$$

This simple but fundamental relation helps to understand the observations we will make.

3 The Results

3.1 Scaling Behavior

Scaling behavior is described by (1). The function $f(q)$ describes the scaling exponents as a function of the order of the moment. It follows from the theory of multi-fractals that this function must be concave Feder (1988). It's general form is an important characteristic of the time series. In the simplest case, $f(q)$ is linear such that $H(q)$ reduces to the (constant) ordinary Hurst exponent H . For a Brownian motion H takes the value $1/2$ while values different from $1/2$ are an indication for anomalous mono-scaling. $H > 1/2$ is found for time series displaying trends on any time scale, while $H < 1/2$ is found for series displaying

| Curr. | Freq. | c_1 | c_2 | $\frac{c_2}{c_1 - 0.5}$ | H(1) | H(2) | γ | R^2 |
|-------|---------|-------|----------|-------------------------|------|-------|----------|-------|
| AUD | (daily) | 0.695 | -0.0975 | 0.500 | 0.61 | 0.560 | 0.5627 | 0.201 |
| | (hf) | 0.583 | -0.01644 | 0.198 | 0.57 | 0.555 | 0.1213 | 0.013 |
| CAD | (daily) | 0.644 | -0.01807 | 0.125 | 0.62 | 0.605 | 0.6454 | 0.395 |
| | (hf) | 0.640 | -0.01462 | 0.104 | 0.64 | 0.615 | 0.8973 | 0.523 |
| DEM | (daily) | 0.661 | -0.02147 | 0.133 | 0.63 | 0.615 | 0.6681 | 0.214 |
| | (hf) | 0.651 | -0.01870 | 0.124 | 0.63 | 0.615 | 1.1965 | 0.559 |
| GBP | (daily) | 0.638 | -0.01467 | 0.106 | 0.62 | 0.605 | 0.8118 | 0.265 |
| | (hf) | 0.637 | -0.01124 | 0.082 | 0.63 | 0.620 | 0.8537 | 0.561 |
| HKD | (daily) | 0.647 | -0.02563 | 0.174 | 0.61 | 0.590 | 0.5157 | 0.190 |
| | (hf) | 0.688 | -0.01695 | 0.090 | 0.69 | 0.660 | 0.9811 | 0.718 |
| JPY | (daily) | 0.608 | -0.01392 | 0.129 | 0.60 | 0.580 | 0.6108 | 0.386 |
| | (hf) | 0.596 | -0.00991 | 0.103 | 0.60 | 0.580 | 0.8143 | 0.600 |
| NLG | (daily) | 0.660 | -0.02066 | 0.129 | 0.63 | 0.615 | 0.5805 | 0.333 |
| | (hf) | 0.640 | -0.01323 | 0.095 | 0.63 | 0.615 | 0.7980 | 0.658 |
| SGD | (daily) | 0.625 | -0.01848 | 0.148 | 0.60 | 0.585 | 0.5041 | 0.291 |
| | (hf) | 0.623 | -0.01647 | 0.134 | 0.62 | 0.600 | 0.8847 | 0.526 |
| USD | (daily) | 0.666 | -0.02366 | 0.143 | 0.63 | 0.615 | 0.7353 | 0.307 |
| | (hf) | 0.689 | -0.01775 | 0.094 | 0.69 | 0.660 | 0.9460 | 0.813 |

Table 1: Behavior of the scaling exponents for log returns of the WSI denominated in different currencies. Both $H(1)$ and $H(2)$ are significantly larger than 0.5. The deviation of the linear part from Brownian-motion scaling ($H = 0.5$) is about ten times larger than the quadratic term. This means that anomalous mono scaling (the mono-fractal part) is the predominant part, and the multi-fractal part can be considered as a higher-order correction. Notice that the scaling exponent of the second moment is significantly larger than 1.

mean-reverting behavior (or anti-trends) on any time scale. A concave form of $f(q)$ indicates multi-scaling or multi-fractal properties.

The scaling behavior $E(|r_\Delta(t)|^q) \sim (\Delta t)^{f(q)}$ of absolute moments $E(|r_\Delta(t)|^q)$ of orders $q \in \{0.2, \dots, 3\}$ persists for about four orders of magnitude. Higher-order moments have not been included in the study because it is not certain that they will exist. The empirical functions $f(q)$ observed for the different cases are displayed in Fig. 1. The continuous lines represent the approximation of the points by the 2nd-order expansion around the point $(0, 0)$,

$$f(q) \equiv qH(q) = c_1q + c_2q^2 + O(q^3).$$

The values of c_1 and c_2 together with $H(1)$ and $H(2)$ are listed in Tab. 1. One notices that the quadratic term is small compared to the linear one. This means that multi-scaling is much less pronounced than the anomaly in the simple scaling. Indeed, for all but one case, the absolute value of c_2 is less than 5% of the value of the corresponding linear coefficient c_1 , and about 10%...20% of the difference of $c_1 - 1/2$, see Tab. 1. It is noteworthy that the scaling exponent of the 2nd moment is significantly larger than 1, namely in the range $1.1 \sim 1.2$, which means that $H(2)$ assumes values between 0.55 and 0.6.

The corresponding results for the FX rates are displayed in Fig. 2 and Tab. 2. The important point is that they display stronger multi-scaling properties (larger values of $|c_2/(c_1 - 0.5)|$) resulting in $H(2)$ -values closer to $1/2$.

| Curr. | Freq. | c_1 | c_2 | $\frac{c_2}{c_1 - 0.5}$ | H(1) | H(2) | γ | R^2 |
|-------|---------|-------|-----------|-------------------------|------|-------|----------|-------|
| AUD | (daily) | 0.610 | -0.09060 | 0.823 | 0.54 | 0.485 | -0.1003 | 0.009 |
| | (hf) | 0.470 | -0.02144 | 0.715 | 0.51 | 0.455 | — | 0.039 |
| CAD | (daily) | 0.520 | -0.017676 | 0.884 | 0.51 | 0.485 | -0.2651 | 0.039 |
| | (hf) | 0.504 | -0.03333 | 8.332 | 0.54 | 0.470 | -1.0742 | 0.239 |
| DEM | (daily) | 0.585 | -0.022677 | 0.267 | 0.56 | 0.540 | -0.0033 | 0.000 |
| | (hf) | 0.550 | -0.04467 | 0.893 | 0.53 | 0.470 | — | 0.001 |
| GBP | (daily) | 0.527 | -0.005622 | 0.208 | 0.54 | 0.525 | -0.3722 | 0.217 |
| | (hf) | 0.474 | -0.01836 | 0.706 | 0.51 | 0.465 | — | 0.000 |
| HKD | (daily) | 0.577 | -0.073740 | 0.957 | 0.56 | 0.460 | -1.1771 | 0.535 |
| | (hf) | 0.449 | -0.07366 | 1.444 | 0.52 | 0.370 | -0.2047 | 0.011 |
| JPY | (daily) | 0.637 | -0.035202 | 0.256 | 0.59 | 0.560 | -0.7200 | 0.359 |
| | (hf) | 0.501 | -0.01727 | 17.270 | 0.52 | 0.485 | -0.3271 | 0.061 |
| NLG | (daily) | 0.589 | -0.025653 | 0.288 | 0.56 | 0.540 | -0.0927 | 0.011 |
| | (hf) | 0.545 | -0.04388 | 0.975 | 0.53 | 0.470 | -0.3979 | 0.045 |
| SGD | (daily) | 0.593 | -0.026524 | 0.285 | 0.57 | 0.540 | -0.3157 | 0.033 |
| | (hf) | 0.448 | -0.02041 | 0.392 | 0.53 | 0.460 | -0.0030 | 0.000 |

Table 2: Behavior of the scaling exponents for FX log returns. In many cases the quadratic term I is of the same size as the difference $H - 0.5$. Accordingly the scaling exponent of the first absolute moment is only slightly larger than $1/2$, ($0.51 \sim 0.59$) and in most cases the scaling exponent of the second moment is close to 1.

3.2 Autocorrelation

If the index or FX rates dynamics were following a geometric Brownian motion, then there should be no autocorrelations of log returns. On the other hand, in the presence of scaling with $H(2) > 0.5$ one expects long range dependence with a power law decay Mandelbrot (1997). Indeed, the decay of the autocorrelation function (acf) of log returns is directly related to $H(2)$:

$$C(\tau) = E [(r_\Delta(t + \tau) - \bar{r}_\Delta) (r_\Delta(t) - \bar{r}_\Delta)] \propto \tau^{-\gamma}, \quad (5)$$

where $\gamma = 2(1 - H(2))$ and \bar{r}_Δ denotes the expected value of the log return $r_\Delta(t)$. (For a simple derivation of this result we refer to the appendix.)

For the WSI, the empirical data show non-vanishing autocorrelations with a power law decay for both the intra-day (Fig. 3) and the daily (Fig. 4) samples. The average value of γ is 0.63 ± 0.10 for the daily data and 0.83 ± 0.29 for the hourly data. Even though in most cases the linear regression yields better values for R^2 for the hourly samples, it is for the daily samples that the values of γ are in somewhat better overall agreement with the values of $H(2)$. This is corroborated by Fig. 5. Indeed, for the daily samples one finds an average value of 0.60 ± 0.02 . A box of size $(\bar{H}(2) \pm \Delta H(2)) \times (\bar{\gamma} \pm \Delta \gamma)$ nearly touches the theoretical line. Even though for hourly data the theoretical line crosses the corresponding box (broken lines) nearly in the middle, the larger box size reduces the value of this result.

For both, daily and intra-day FX returns, there is no significant autocorrelation of the log returns: most of the values of the autocorrelation function

| Curr. | Freq. | WSI | | | FX | | |
|-------|---------|---------|-------|----------|---------|-------|----------|
| | | β | R^2 | α | β | R^2 | α |
| AUD | (daily) | 0.1396 | 0.969 | 0.0000 | -0.0171 | 0.088 | 0.2676 |
| | (hf) | 0.0836 | 0.923 | 0.0000 | -0.0732 | 0.923 | 0.0000 |
| CAD | (daily) | 0.2134 | 0.993 | 0.0000 | -0.0227 | 0.020 | 0.4168 |
| | (hf) | 0.1684 | 0.984 | 0.0000 | -0.0618 | 0.892 | 0.0000 |
| DEM | (daily) | 0.2430 | 0.985 | 0.0000 | 0.0945 | 0.844 | 0.0000 |
| | (hf) | 0.1509 | 0.991 | 0.0000 | -0.0355 | 0.591 | 0.0014 |
| GBP | (daily) | 0.2222 | 0.990 | 0.0000 | 0.0558 | 0.738 | 0.0000 |
| | (hf) | 0.1683 | 0.990 | 0.0000 | -0.0412 | 0.965 | 0.0000 |
| HKD | (daily) | 0.2015 | 0.985 | 0.0000 | -0.0321 | 0.141 | 0.0000 |
| | (hf) | 0.2238 | 0.994 | 0.0000 | -0.3386 | 0.938 | 0.0000 |
| JPY | (daily) | 0.1790 | 0.983 | 0.0000 | 0.1188 | 0.916 | 0.0000 |
| | (hf) | 0.1064 | 0.990 | 0.0000 | -0.0140 | 0.023 | 0.2119 |
| NLG | (daily) | 0.2458 | 0.984 | 0.0000 | 0.0897 | 0.891 | 0.0000 |
| | (hf) | 0.1751 | 0.996 | 0.0000 | -0.0346 | 0.534 | 0.0013 |
| SGD | (daily) | 0.2001 | 0.973 | 0.0000 | 0.0435 | 0.099 | 0.1515 |
| | (hf) | 0.1354 | 0.978 | 0.0000 | -0.0628 | 0.704 | 0.0000 |
| USD | (daily) | 0.2279 | 0.994 | 0.0000 | — | — | — |
| | (hf) | 0.2285 | 0.995 | 0.0000 | — | — | — |

Table 3: Scaling behavior of the quadratic variation. Notice that for the WSI the scaling exponent is positive with very high significance. This means that the quadratic variation vanishes in the limit $\Delta t \rightarrow 0$. For FX data, the hypothesis of positive scaling exponents must be rejected.

(acf) cannot be significantly distinguished from white noise, so that any further analysis is not meaningful.

3.3 Quadratic Variation

Quadratic variation is of central interest for stochastic processes in finance. For a time-continuous process X_t this quantity is defined as

$$[X]_t := \lim_{\|P\| \rightarrow 0} \sum_{k=1}^n (X(t_k) - X(t_{k-1}))^2 \quad (6)$$

where P ranges over all partitions of the interval $[0, t]$, the norm $\|P\|$ denotes the length of the longest subinterval, $\|P\| = \max_k (t_k - t_{k-1})$, and the limit is defined in the sense of convergence in probability.

As we work with regular time series, $\|P\| = \Delta$ such that (6) can be rewritten as

$$[X]_t = \lim_{n \rightarrow \infty} \sum_{k=1}^n (r_\Delta(t_k))^2 \quad (7)$$

with $r_\Delta(t_k) = X(t_0 + k\Delta) - X(t_0 + (k-1)\Delta)$. Notice that Δ and $n = n(\Delta)$ are related by $n = t/\Delta$. If $X(t)$ is a series of log prices then $r_\Delta(t)$ is the log return at time t with respect to the step size (or time horizon) Δ . When the log returns are stationary and uncorrelated, $[X]_t$ is directly related to the scaling of the second

moment. Indeed, for large n one can approximate the sum along the path by the expectation, $\sum_{k=1}^n (r_\Delta(t_k))^2 \simeq n E((r_\Delta(t_k))^2)$ such that the approximation of the quadratic variation by a regular time series with time step Δ reads

$$[X]_t^{(\Delta)} = \sum_{k=1}^{n(\Delta)} (r_\Delta(t_k))^2 = \frac{t}{\Delta} E((r_\Delta(t_k))^2) \propto \frac{t \Delta^{f(2)}}{\Delta} \propto \Delta^\beta \quad (8)$$

with $\beta = f(2) - 1$. Thus, when $f(2) = 1$ the finite time-step approximation of the quadratic variation does not depend on Δ in the $\Delta \rightarrow 0$ limit, while it tends to 0 for $f(2) > 0.5$ and to ∞ for $f(2) < 0.5$.

The important message of our analysis is that for the WSI in all currency denominations investigated the finite-step approximation $[X]_t^{(\Delta)}$ of the quadratic variation tends to zero for $\Delta \rightarrow 0$. For FX rates, on the other hand, the picture is mixed. In a number of cases the null hypothesis of a scaling exponent of $\beta = 0$ cannot be rejected at the 1% significance level, see Tab. 3. In the cases when there are significant deviations these are either negative or positive. In addition, the β -values obtained for the daily and the corresponding intra-day series differ ones from the others. All significant deviations of intra-day series have negative scaling exponents while in the case of the daily series all but one significant deviations are positive. The difference may be caused by the fact that at very small time steps market microstructure effects play a role.

Only the Hong Kong dollar is strongly out of line, displaying a negative β -value for both the daily and the intra-day series. The strongly mean-reverting behavior implied by the particularly small value of $\beta = -0.34$ for the intra-day series can be explained by the fact that the HKD is pegged to the US dollar, leading to frequent interventions of the Hong Kong Monetary Authority when the exchange rate approaches the limits of the allowed band. Similar behavior has been reported for the European currencies tied together in the European Monetary System during the ninetieth of the last century Dacorogna et al. (2001).

3.4 Shapes of the Return Distributions

For characterizing the return distributions $f_R(r)$ the empirically observed log-returns r have been fitted with generalized hyperbolic (GH) distributions by means of maximum-likelihood estimation for all data sets. GH distributions, which have been introduced by Barndorff-Nielsen & Blaesild (1981) and Barndorff-Nielsen (1978), provide an excellent class of distributions to faithfully parameterize the great majority of return distributions encountered in financial markets Eberlein & Keller (1995), Eberlein, Keller & Prause (1998), Bibby & Sørensen (2003), McNeil, Frey & Embrechts (2005). Their role in financial modeling is discussed e.g. in Bingham & Kiesel (2002). They belong to the class of mean-variance mixture distributions whose density is given as

$$f_R(r) = \int_0^\infty \frac{e^{\frac{r-\mu}{\sigma^2}\gamma}}{\sqrt{2\pi}\sigma} \exp\left\{-\frac{(r-\mu)^2}{2\sigma^2} \frac{1}{w} - \frac{1}{2} \frac{\gamma^2}{\sigma^2} w\right\} h(w) dw. \quad (9)$$

Here μ and σ are location and scale parameters and γ denotes the skewness parameter. For the class of generalized hyperbolic distributions h denotes the

generalized inverse Gaussian density

$$h(w) = \left(\frac{\psi}{\chi}\right)^{\lambda/2} \frac{w^{\lambda-1}}{2K_{\lambda}(\sqrt{\chi\psi})} \exp\left\{-\frac{1}{2}\left(\frac{\chi}{w} + \psi w\right)\right\}. \quad (10)$$

The closed form density of the GH distribution in this parametrization can be found in McNeil, Frey & Embrechts (2005). The degree of freedom arising in this particular mixture representation — also mentioned in (McNeil, Frey & Embrechts 2005, Chapter 3) — is eliminated through the constraint $E(W) = 1$, which substitutes χ and ψ by the sole shape-parameter $\bar{\alpha}$ through the relationship

$$\chi = \bar{\alpha} \frac{K_{\lambda}(\bar{\alpha})}{K_{\lambda+1}(\bar{\alpha})}, \quad \psi = \frac{\bar{\alpha}^2}{\chi} = \bar{\alpha} \frac{K_{\lambda+1}(\bar{\alpha})}{K_{\lambda}(\bar{\alpha})}. \quad (11)$$

The GH class comprises distributions of the following types: variance gamma (also called generalized Laplace distribution Kotz, Kozubowski & Podgórski (2001)), hyperbolic Bibby & Sørensen (1997), normal inverse Gaussian Barndorff-Nielsen (1997), and Student- t . They are consistent with different types of processes used for modeling the price dynamics, e.g. Lévy-processes Raible (2000), Barndorff-Nielsen (1998), Barndorff-Nielsen & Shephard (2008) and the Minimal Market Model Platen & Heath (2006). GH distributions have semi-heavy tails with the exception of the Student- t limiting case, which has heavy tails.

The values of the shape parameters $\bar{\alpha}$ and λ are shown in Fig. 6 for the WSI (top) and the FX rates (bottom) fitted to symmetric (left) and skewed (right) GH distributions. In this plot, the deviation from the normal distribution increases with decreasing distance from the center of the coordinate system. I.e., the normal distribution is obtained in the $|\lambda| \rightarrow \infty$ or/and $\bar{\alpha} \rightarrow \infty$ limit. The upper $\bar{\alpha} = 0$ half line represents the variance gamma (VG) distribution and the lower half line represents the Student- t distribution with $\nu = -2\lambda$ degrees of freedom. Notice that the $\bar{\alpha}$ -axis is plotted on a logarithmic scale, which enlarges very short distances from the $\bar{\alpha} = 0$ line. The WSI currency denominations, resp. FX rates, are encoded by the colors of the symbols and the time horizons by their shapes, the unfilled forms being used for small time horizons and the filled ones for long horizons. The density is represented on a log scale and color-encoded, light colors indicating high densities and dark colors indicating low densities.

The overall shape of the sets of points is similar for the fit with symmetric distributions (left) and skewed distributions (right), while the shape is different for WSI returns (top) and FX returns (bottom). For the WSI there is a significant concentration of points for $\bar{\alpha}$ practically zero or very small and λ either between 1 and 2 (VG) for the very short horizons of the order of an hour or less and between -2 and -3 (Student- t distribution between 4 and 6 degrees of freedom) for the very long time horizons of up to several months; on average there is a smooth transition from one limiting case to the other passing on a curved line. This is in line with results reported for intra-day Breyman, Kelly & Platen (2006) and daily Fergusson & Platen (2006) data. Let us recall that the Student- t distribution is the only limiting case displaying heavy tails. The log returns remain t -distributed with degrees of freedom between 4 and 6 when the time horizon is increased up to several months. This means that there is no transition from heavy-tailed return distributions to normal distributions when enlarging the time horizon, contrary to what has been suggested by other findings.

In the FX case, the shape of the set of points is much less structured. In any case, for small time steps the points cluster at small but positive λ -values and very small $\bar{\alpha}$ -values and there is a continuous transition from these small parameter values to larger $\bar{\alpha}$ and $|\lambda|$ values. This transition indicates the progressive change in shape with increasing time horizon towards a normal distribution, which is in line with the multi-scaling properties discussed above.

3.5 Dependence Structure

To get an idea about the influence of the dependence structure, we investigated the bivariate densities of (i) WSI log returns in two different denominations (see Figs. 7 and 9) and (ii) different FX log returns (see Figs. 8 and 10). Figure 7 shows the densities for daily WSI returns, where for all plots the scales of the axes are the same. The following facts are striking:

- (i) In all denominations the volatility is approximately the same;
- (ii) the principal axes are all aligned along the diagonal;
- (iii) the densities seem to be composed of an elliptical contour, with some extrem events (jumps) principally located on the diagonal; and
- (iv) there are more downward jumps than upward jumps.

The first two facts imply that the daily WSI dynamics is driven by the dynamics of the local indices and not by the FX rates. Indeed, the log return $r_{\Delta}^{I_j}(t)$ with horizon Δ of the WSI denominated in currency j is just the sum of the WSI log return denominated in USD plus the log return of the USD/ j FX rate:

$$r_{\Delta}^{I_j}(t) = r_{\Delta}^{I_{\text{USD}}}(t) + r_{\Delta}^{\text{USD}/j}(t). \quad (12)$$

The fact that on any single plot the principal axes is aligned along the diagonal means that either all FX rates must be under the same influence or they have nearly no influence on the WSI at all. From the density plots of the FX rates (see Figs. 8 and 10) it follows that the latter is the case. Similarly, the alignment of the jumps on the diagonals indicates that they originate in the stock market and not in the FX market. Fact (iv) will impact the scaling properties.

The bivariate densities of the FX rates in Fig. 8 look quite differently. In that plot the axes have different scales since otherwise the densities could not have been well represented. The ratio of the scales on the x - and y -axes can be deduced from the inclination of the diagonals depicted by black straight lines. The following observations are important:

- (v) The FX returns display different volatilities
- (vi) The principal axes are typically not aligned along diagonals
- (vii) No clear pattern for the location of extreme events can be distinguished.

These three facts together imply that on a daily time scale FX rates behave quite idiosyncratic, for both small events and extreme events.

This is already a hint towards the origin of the different scaling behavior of FX and WSI returns. To look into this in some more detail, we write the FX log

return as the difference of the log returns of the index in these denominations:

$$r_{\Delta}^{j/k}(t) = r_{\Delta}^{I_k}(t) - r_{\Delta}^{I_j}(t). \quad (13)$$

The scaling behavior of the FX return is thus expressed in terms of the index returns as

$$E \left[\left| r_{\Delta}^{j/k}(t) \right|^q \right] = E \left[\left| r_{\Delta}^{I_k}(t) - r_{\Delta}^{I_j}(t) \right|^q \right]. \quad (14)$$

It is clear that the right-hand-side of this equation strongly depends on the dependence structure of the different denominations of the index. Qualitatively, if a jump occurs in one of the regional stock markets this results in a jump of the WSI that in any denomination has the same size and thus cancels out in the difference at the right-hand-side of (14). Jumps originating from the FX market, on the other hand, will affect different denominations of the WSI differently. If stock market jumps are more frequent and/or larger than FX jumps (as is suggested by Figs. 7 and 8) this will lead to differences in the scaling behavior and could explain the different values of $f(2)$ for the WSI and FX rates.

At the 5 min observation time step size displayed in Figs. 9 and 10 things look quite differently. Here, again, the WSI return densities are all plotted with the same scales of the axes, indicating similar volatility, while for the FX densities different scales had to be chosen for different plots, meaning that volatility is different for different rates. It is striking that now both principal axes as well as the extremes are aligned with the x and/or y axes. This is true for both the WSI as well as the FX returns. This observation means the following:

- (viii) At the 5 min horizon there are very few correlations among the WSI returns in different denominations and among different FX rates, and
- (ix) jumps originate in the FX returns and not in the stock markets (because otherwise, in Fig. 9 they should be located on the diagonal and not along the axes).

4 Discussion and Conclusion

The following facts have been observed:

- Different scaling properties in WSI returns versus FX returns, leading to power law decay of the autocorrelation function (acf) of WSI log returns while acf of FX log returns vanishes, and to vanishing quadratic variation in the $\Delta \rightarrow 0$ limit.
- The WSI displays variance-gamma distributed log returns for small time horizons, which successively transform into Student- t distributed log returns for larger observation time step sizes. For FX, semi-heavy tails at very short time steps have been observed, which successively become more normal-distributed like for larger time steps.
- Jumps observed in the intra-day WSI data at the 5 min horizon originate in the FX market, while jumps observed in the daily WSI data at the daily horizon originate in the stock markets. For the daily step size, jumps in the stock market do hardly reflect the FX market.

From these observations the following overall image emerges. The multi-fractal properties of the FX market are likely driven by jumps that are idiosyncratic for the FX market (or at least do not originate in the stock markets). These jumps are rather small and occur at the high frequency level, thus leading to a transition from distributions with pronounced tails to a normal-distribution. This implies the observed seemingly multi-fractal scaling behaviour. Even though this kind of behaviour can be described by a cascade from long to short time horizons as claimed in Ghashghaie et al. (1996) and modeled by different cascade-based processes Muzy, Delour & Bacry (2000), Bacry, Delour & Muzy (2001), Calvet & Fisher (2001, 2002), it is not clear that such a process is at the origin of the observed facts. The results presented here give hints in the directions that the driving events are the high-frequency small jumps and that larger jumps play a minor role. However, this does not exclude the possibility that larger jumps from whatever source including the stock markets may be at the origin of a cascade that eventually results in the high-frequency small jumps observed in the density plots. In this way the results presented here could be compatible with the observation in ref. Arneodo, Muzy & Sornette (1998) of a causal cascade from long to short time horizons. Further research is needed to confirm this picture.

The interesting scaling properties of the WSI, together with the absence of a transition of the return distribution towards a normal-distribution for large observation time steps, is likely to be caused by a combination of events. On one hand, the high-frequency small jumps driving the FX dynamics do appear in the WSI. At larger (daily and longer) time horizons, jumps occur in the stock markets. These jumps are larger and less frequent. There may even be a hierarchy of jumps which is required to generate the almost mono-scaling behaviour. The existence of such a hierarchy is suggested by the fact that the stock market is driven by information on a weekly, monthly or even quarterly scale with groups of market participants acting on a similar time scale. Such a process would be able to generate the observed scaling behaviour and thus also the observed behaviour of the quadratic variation, even though it could still be described in the framework of jump-diffusion processes.

At the current state, however, it is not certain that the empirical behaviour of WSI returns presented here is entirely caused by jumps. Delay effects, which may be caused by the time needed for institutional or other groups of investors to react to the information and rebalance their portfolio, may likewise play a role. To clarify these points, further research is needed.

As to the theoretical description, it is too early to say which kind of approach will eventually prevail. The convincing integration of the above-mentioned empirical findings on financial market data into a unifying theoretical framework for the entire financial market is still missing. Mathematical theories which aim at a generalization of standard processes towards Lévy processes and fractional Brownian motion, are typically formulated for a single asset, and are still in their infancy as far as modeling the entire market dynamics is concerned Barndorff-Nielsen & Shephard (2008). What we have shown in the current paper is that a broadly diversified index has a much better signal to noise ratio than, e.g., stock prices or exchange rates. The diversification effect provides cleaner statistical properties for an index, which has shown to be very useful to disentangle

otherwise bewildering facts.

Acknowledgement

We thank R. Locher for valuable comments concerning the presentation of the data and Renata Rendek for her inspiring remarks. This research has been financially supported by the COST P10 action and Swiss SER grant no. C05.0039.

Appendix

A: Return Autocorrelation Functions for Multi-fractal Price Series

Let Δ denote the elementary time step, e.g. the sampling period. The return with lag k is defined as

$$r_k(t) = x(t) - x(t - k\Delta). \quad (15)$$

From the aggregation property of returns, $r_k(t) = \sum_{i=0}^{k-1} r_1(t - i\Delta)$ and the ‘‘stationarity’’ of $r_i(\cdot)$ it immediately follows that

$$E(r_{k+1}(t)^2) = E(r_k(t)^2) + E(r_1(t)^2) + 2 \sum_{i=0}^{k-1} E(r_1(t - k\Delta)r_1(t - i\Delta)) \quad (16)$$

The acf for a process with zero mean is defined as

$$C(i) = \frac{E(r_1(t)r_1(t - i))}{E(r_1(t)^2)}. \quad (17)$$

This means that the terms under the summation sign in (16) can be expressed as acf, which leads to

$$E(r_{k+1}(t)^2) = E(r_k(t)^2) + E(r_1(t)^2) + 2 E(r_1(t)^2) \sum_{i=0}^{k-1} C(k - i). \quad (18)$$

Making use of the scaling law

$$E(r_k(t)^2) = A k^{f(2)} \quad (19)$$

yields the relation

$$(k + 1)^{f(2)} = k^{f(2)} + 1 + 2 \sum_{i=0}^{k-1} C(k - i). \quad (20)$$

It can now be shown by complete induction that $C(k)$ has the form

$$C(k) = \frac{(k + 1)^{f(2)}}{2} - k^{f(2)} - \frac{(k - 1)^{f(2)}}{2}. \quad (21)$$

For $n = 1$ this relation follows directly from (20). Now let us assume that (21) is true up to a certain $k = n$. Then for $k = n + 1$ solving (20) for $C(n + 1)$ yields

$$C(n + 1) = \frac{(n + 2)^{f(2)} - (n + 1)^{f(2)} - 1}{2} - \sum_{i=1}^n C(n + 1 - i). \quad (22)$$

By means of (20) the sum can be rewritten as

$$\sum_{i=1}^n C(n + 1 - i) = C(n) + \sum_{i=1}^{n-1} C(n - i) = \frac{(n + 1)^{f(2)} - (n)^{f(2)} - 1}{2}.$$

Inserting this into (21) proves the proposition.

The asymptotic behavior ($k \gg 1$) can be found by expanding the right-hand-side of (21) up to second order around k . The first-order terms cancel, such that the final result is

$$C(\tau) = 2H(2)(2H(2) - 1)\tau^{2H-2}, \quad (23)$$

where $\tau = k\Delta$.

References

- Arneodo, A., J. F. Muzy, & D. Sornette (1998). “Direct” causal cascade in the stock market. *European Physical Journal B* **2**, 277–282.
- Bacry, E., J. Delour, & J. F. Muzy (2001). Multifractal random walk. *Phys. Rev. E* **64**(2), 0261031–0261034.
- Barndorff-Nielsen, O. (1978). Hyperbolic distributions and distributions on hyperbolae. *Scand. J. Statist.* **5**, 151–157.
- Barndorff-Nielsen, O. (1997). Normal inverse Gaussian distributions and stochastic volatility modelling. *Scand. J. Statist.* **24**, 1–13.
- Barndorff-Nielsen, O. (1998). Processes of normal inverse Gaussian type. *Finance Stoch.* **2**(1), 41–68.
- Barndorff-Nielsen, O. & P. Blaesild (1981). Hyperbolic distributions and ramifications: Contributions to theory and application. In C. Taillie, G. P. Patil, and B. A. Baldessari (Eds.), *Statistical Distributions in Scientific Work*, Volume 4, pp. 19–44. Dordrecht: Reidel.
- Barndorff-Nielsen, O. & N. Shephard (2008). *Continuous Time Approach to Financial Volatility*. Cambridge University Press, Cambridge.
- Bartolozzi, M., D. Leinweber, & A. Thomas (2005). Stochastic opinion formation in scale-free networks. *Physica A: Statistical Mechanics and its Applications* **350**(2-4), 451–.
- Bibby, B. M. & M. Sørensen (1997). A hyperbolic diffusion model for stock prices. *Finance Stoch.* **1**, 25–41.
- Bibby, B. M. & M. Sørensen (2003). Hyperbolic processes in finance. In S. T. Rachev (Ed.), *Handbook of Heavy Tailed Distributions in Finance*, pp. 211–248. Elsevier, Amsterdam.

- Bingham, N. H. & R. Kiesel (2002). Semi-parametric modelling in finance: Theoretical foundations. *Quant. Finance*. **2**(4), 241–250.
- Breymann, W. (2000). Dynamic theta time: Algorithm, configuration, tests. Internal document WAB.2000-07-31, Olsen & Associates, Seefeldstrasse 233, 8008 Zürich, Switzerland.
- Breymann, W. (2002). *hffinance*, Available from URL <https://home.zhaw.ch/~bwlf/>.
- Breymann, W., A. Dias, & P. Embrechts (2003). Dependence structures for multivariate high-frequency data in finance. *Quant. Finance*. **3**(1), 1–14.
- Breymann, W., S. Ghashghaie, & P. Talkner (2000). A stochastic cascade model for FX dynamics. *Int. J. Theor. Appl. Finance* **3**(3), 357–360.
- Breymann, W., L. Kelly, & E. Platen (2006). Intraday empirical analysis and modeling of diversified world stock indices. *Asia-Pacific Financial Markets* **12**(1), 1–28.
- Calvet, L. & A. Fisher (2001). Forecasting multifractal volatility. *J. Econometrics* **105**, 27–68.
- Calvet, L. & A. Fisher (2002). Multifractality in asset returns: theory and evidence. *Rev. Econom. Statist.* **84**(3), 381–406.
- Dacorogna, M., R. Gençay, U. Müller, R. Olsen, & O. Pictet (2001). *An Introduction to High-Frequency Finance*. Academic Press, San Diego, CA.
- Eberlein, E. & U. Keller (1995). Hyperbolic distributions in finance. *Bernoulli* **1**, 281–299.
- Eberlein, E., U. Keller, & K. Prause (1998). New insights into smile, mispricing, and value at risk: The hyperbolic model*. *J. Business* **71**(3), 371–405.
- Feder, J. (1988). *Fractals, Physics of Solids and Liquids*. Plenum Press.
- Fergusson, K. & E. Platen (2006). On the distributional characterization of log-returns of a world stock index. *Appl. Math. Finance* **13**(1), 19–38.
- Ghashghaie, S., W. Breymann, J. Peinke, P. Talkner, & Y. Dodge (1996). Turbulent cascades in foreign exchange markets. *Nature* **381**, 767–770.
- Kotz, S., T. Kozubowski, & K. Podgórski (2001). *The Laplace Distribution and Generalizations*. Birkhäuser.
- Le, T. & E. Platen (2006). Approximating the growth optimal portfolio with a diversified world stock index. *J. Risk Finance* **7**(5), 559–574.
- Mandelbrot, B. (1963). The variation of certain speculative prices. *J. Business* **36**, 394–419. Reprinted in Cootner (1964), Chapter 15, 307–337.
- Mandelbrot, B. (1997). *Fractals and Scaling in Finance*. Springer.
- Mandelbrot, B. (2001a). Scaling in financial prices: I. Tails and dependence. *Quant. Finance*. **1**, 113–123.
- Mandelbrot, B. (2001b). Scaling in financial prices: II. Multifractals and the star equation. *Quant. Finance*. **1**, 124–130.
- Mandelbrot, B. (2001c). Scaling in financial prices: III. Cartoon Brownian motions in multifractal time. *Quant. Finance*. **1**(4), 427–.
- Mandelbrot, B. (2001d). Scaling in financial prices: IV. Multifractal concentration. *Quant. Finance*. **1**, 641–649.

- Mantegna, R. N. & H. E. Stanley (1995). Scaling behaviour in the dynamics of an economic index. *Nature* **376**, 46–49.
- Mantegna, R. N. & H. E. Stanley (1997). Stock market dynamics and turbulence: Parallel analysis of fluctuation phenomena. *Physica A* **239**, 255–266.
- Matteo, T. D. (2007). Multi-scaling in finance. *Quant. Finance*. **7**(1), 21–36.
- Matteo, T. D., T. Aste, & M. Dacorogna (2003). Scaling behaviors in differently developed markets. *Physica A* **324**, 183–188.
- Matteo, T. D., T. Aste, & M. Dacorogna (2005). Long-term memories of developed and emerging markets: Using the scaling analysis to characterize their stage of development. *J. Banking and Finance* **29**(4), 827–851.
- McNeil, A., R. Frey, & P. Embrechts (2005). *Quantitative Risk Management*. Princeton University Press.
- Müller, U., M. Dacorogna, R. B. Olsen, O. Pictet, M. Schwarz, & C. Morgenegg (1990). Statistical study of foreign exchange rates, empirical evidence of a price change scaling law, and intraday analysis. *J. Banking and Finance* **14**(6), 1189–1208.
- Muzy, J., J. Delour, & E. Bacry (2000). Modelling fluctuations of financial time series: from cascade process to stochastic volatility model. *European Physical Journal B* **17**(3), 537–548.
- Platen, E. & D. Heath (2006). *A Benchmark Approach to Quantitative Finance*. Springer Finance. Springer.
- Raible, S. (2000). *Levy processes in finance: Theory, numerics and empirical facts*. Ph. D. thesis, Universität Freiburg i. Br., <http://deposit.ddb.de/cgi-bin/dokserv?idn=961285192>.
- Struzik, Z. R. & K. Kiyono (2006). Criticality and phase transition in stock-price fluctuations. *Phys. Rev. Letters* **96**, 068701–.

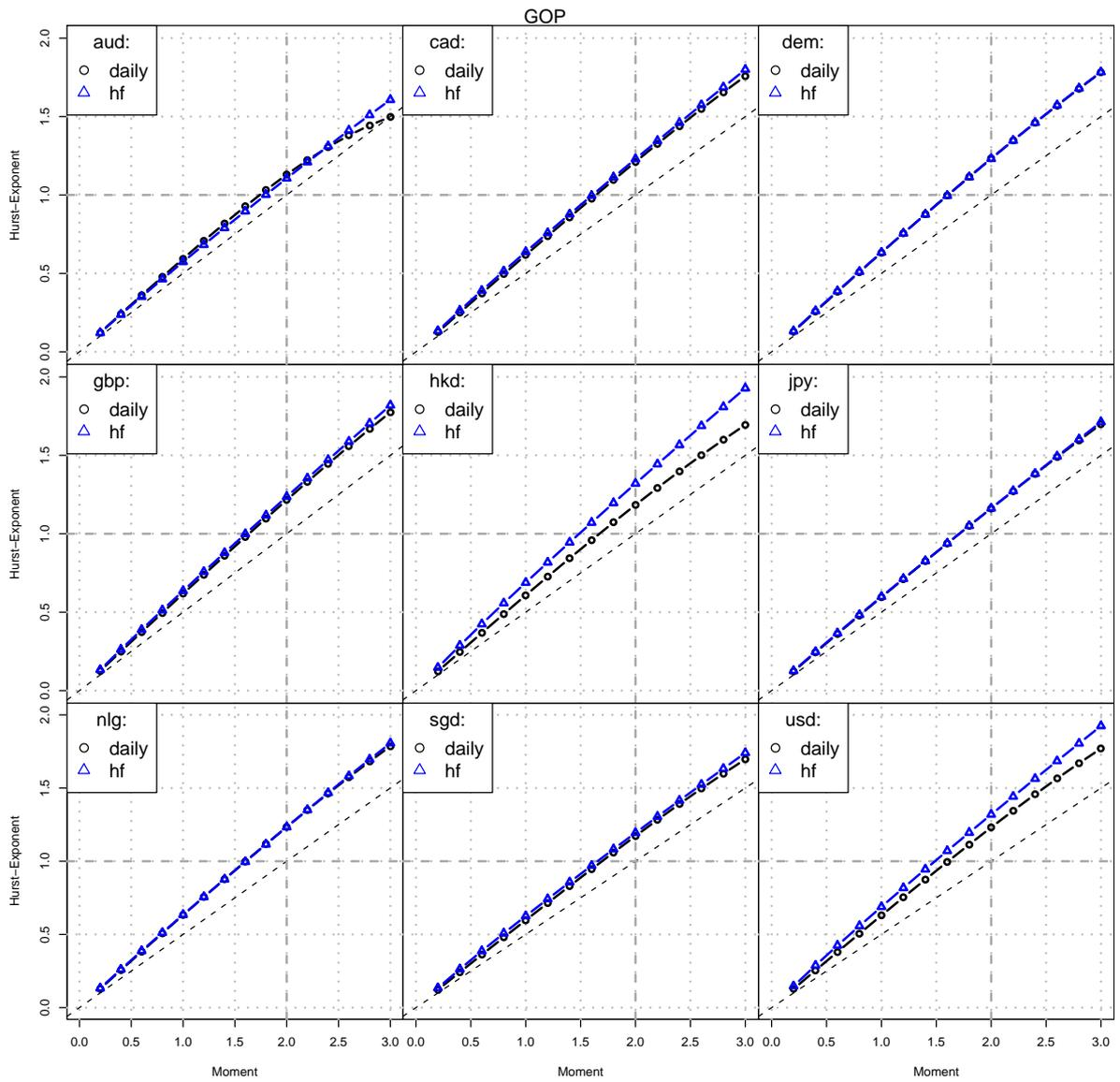


Figure 1: Scaling exponents $f(q)$ as function of the order q of the absolute moment of WSI log returns.

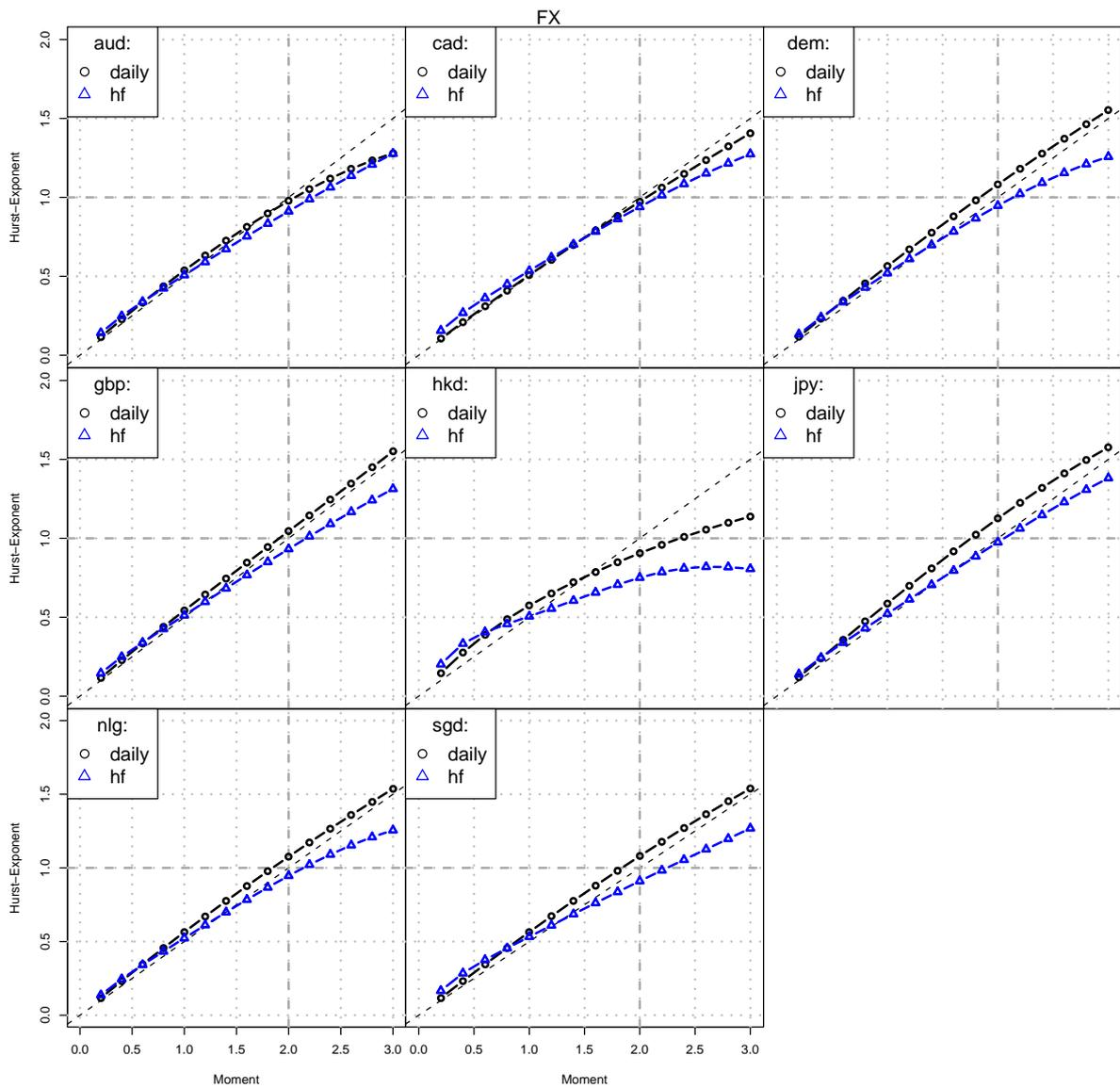


Figure 2: Same as Fig. 1 for FX log returns.

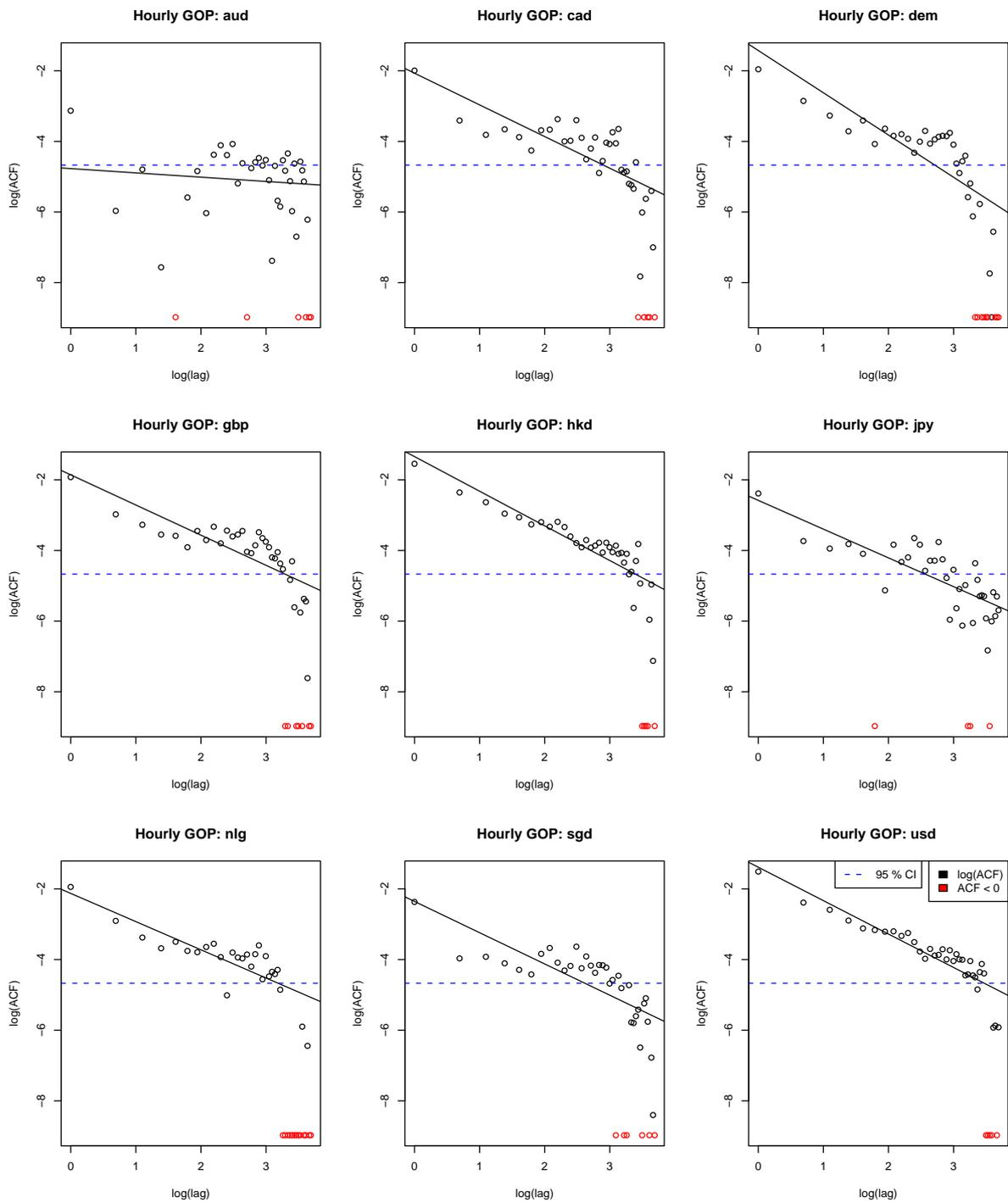


Figure 3: Log-log plot of the acf of hourly WSI log returns. Negative values, which cannot be represented on the log-scale, are indicated by red points at the bottom of each plot.

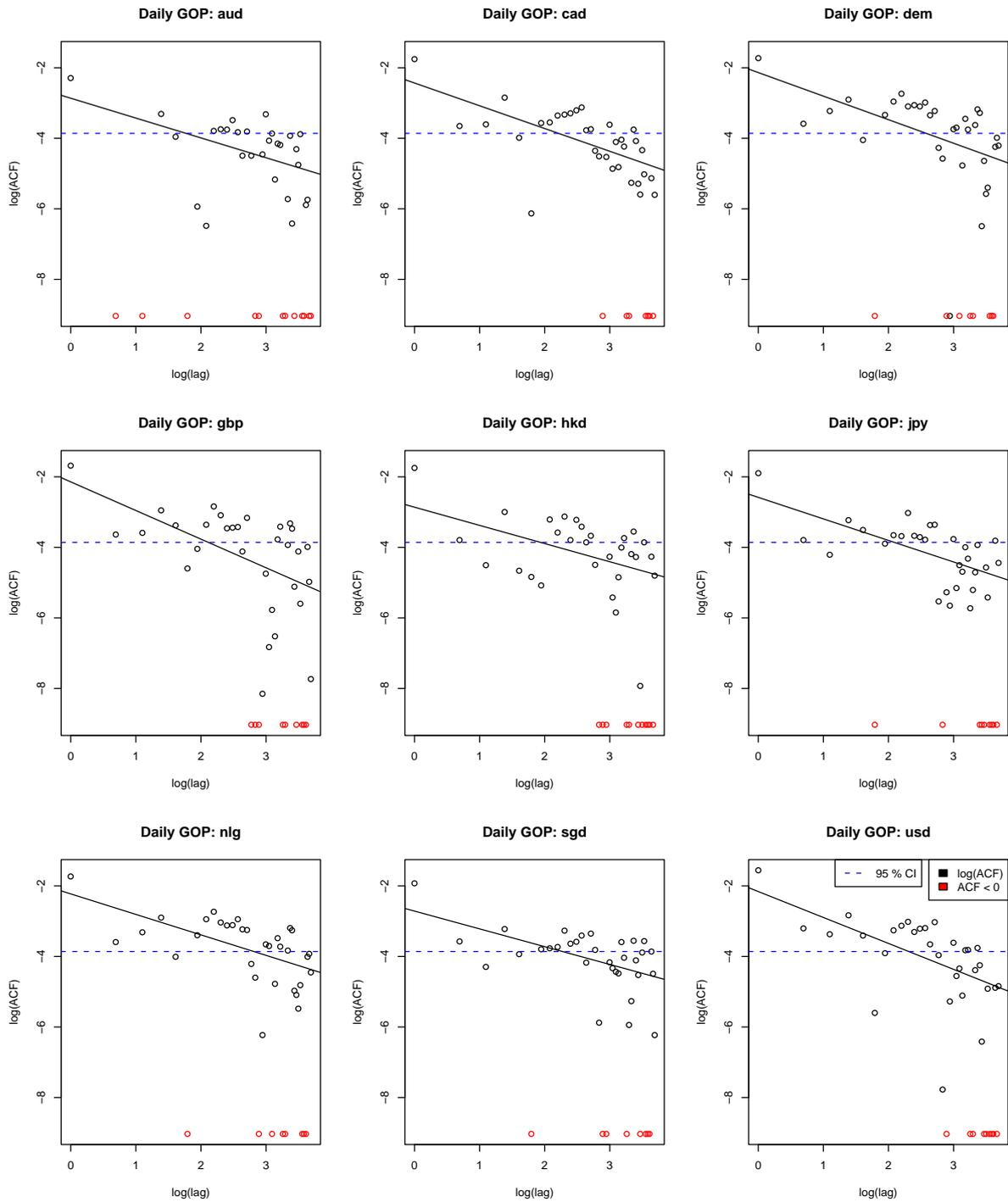


Figure 4: Same as Fig. 3 for daily WSI log returns.

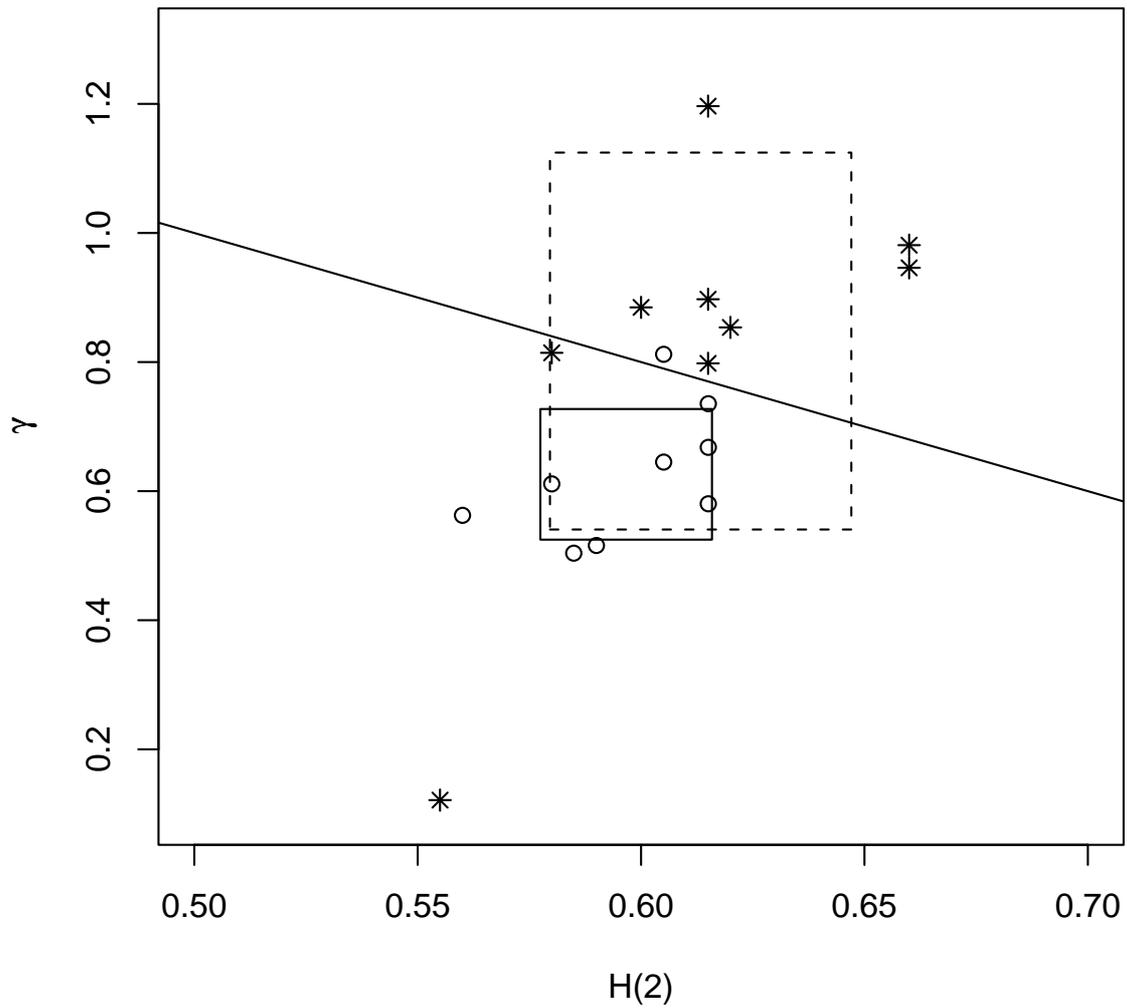


Figure 5: Decay exponents γ of the acf's as a function of the Hurst exponent $H(2)$ for WSI log returns. Circles: daily returns; stars: hourly returns. The black line indicates the relationship $\gamma = 2(1 - H(2))$. The size of the boxes is ± 1 standard deviation from the average of the respective quantities. Continuous line: daily data; broken line: hourly data.

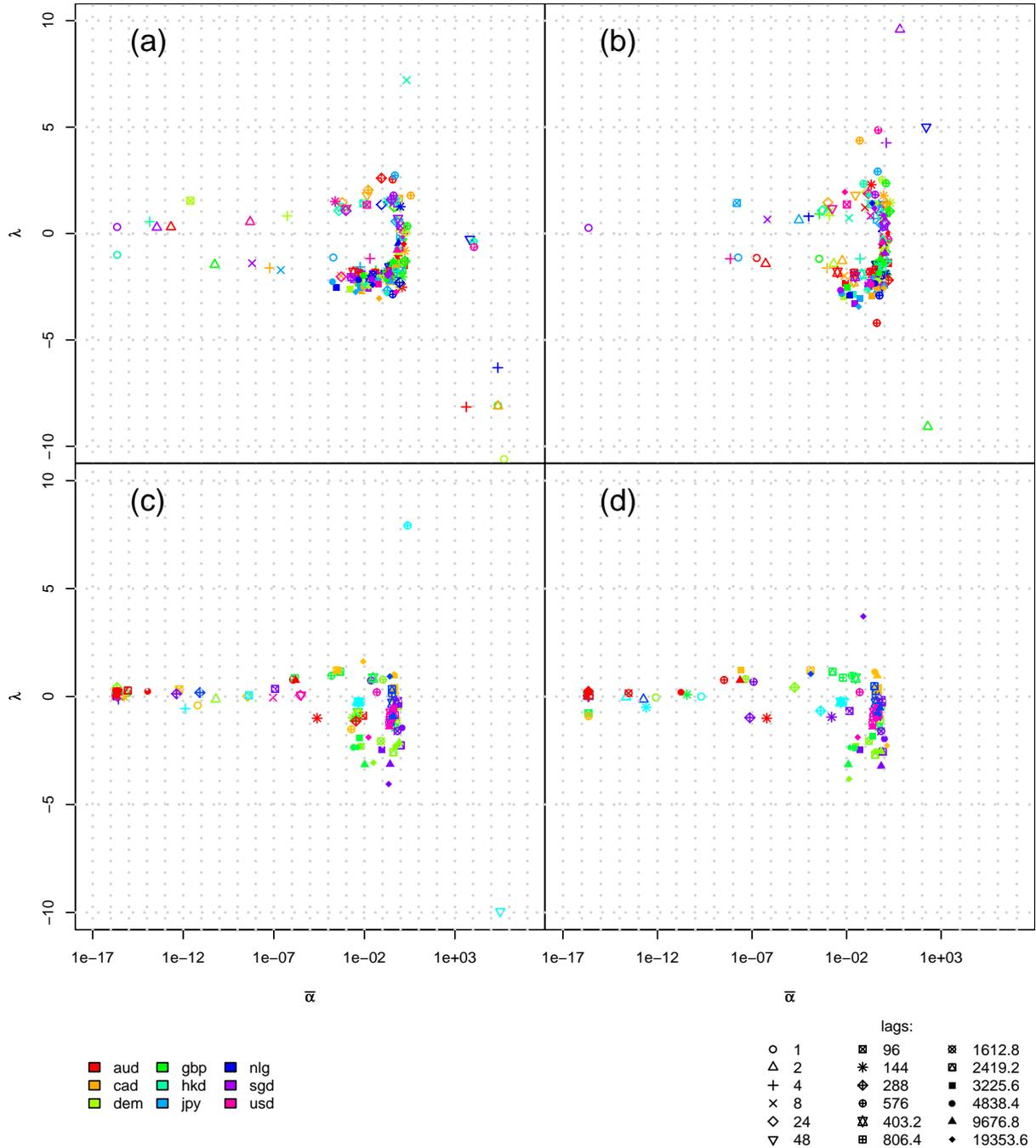
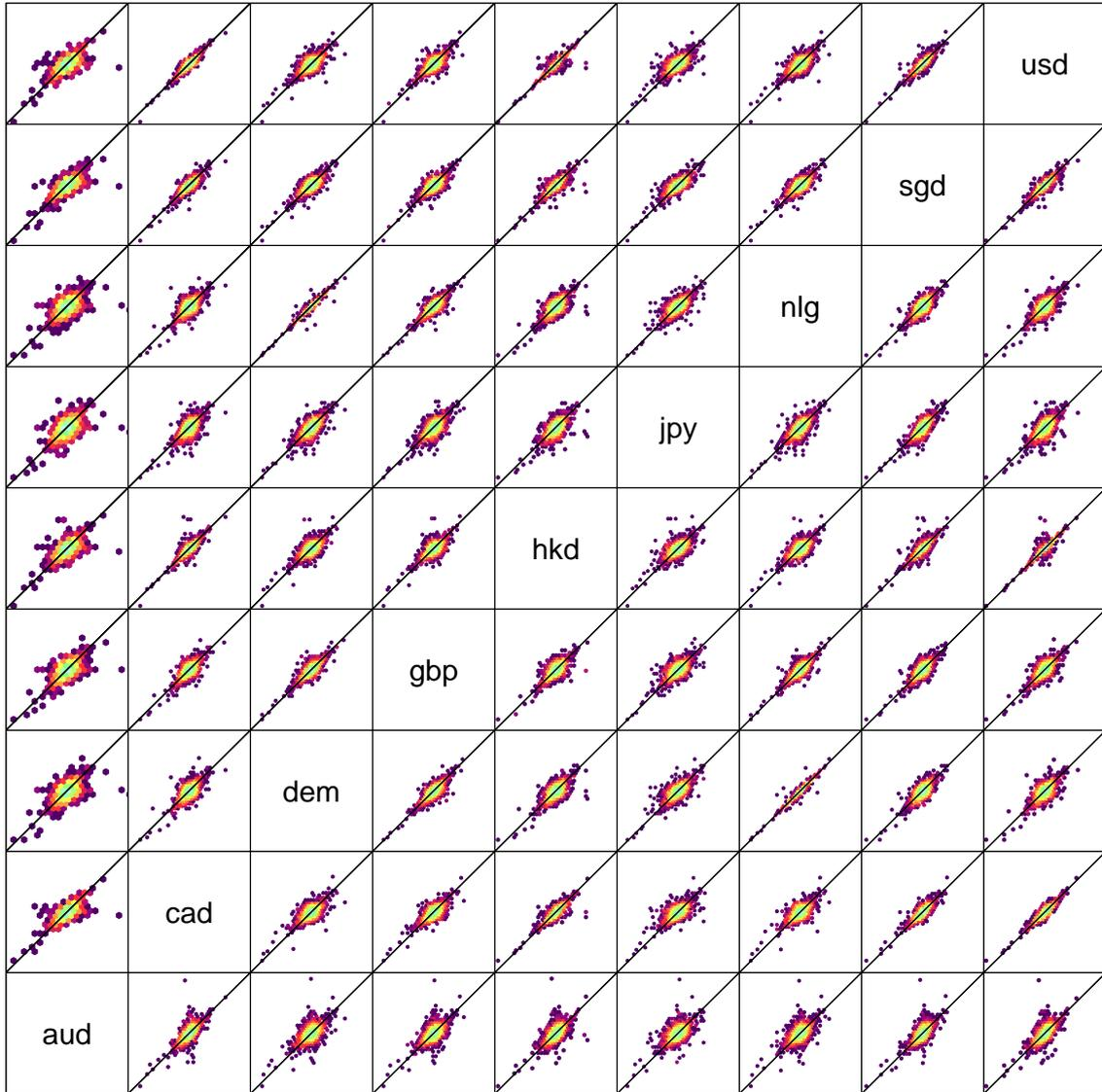
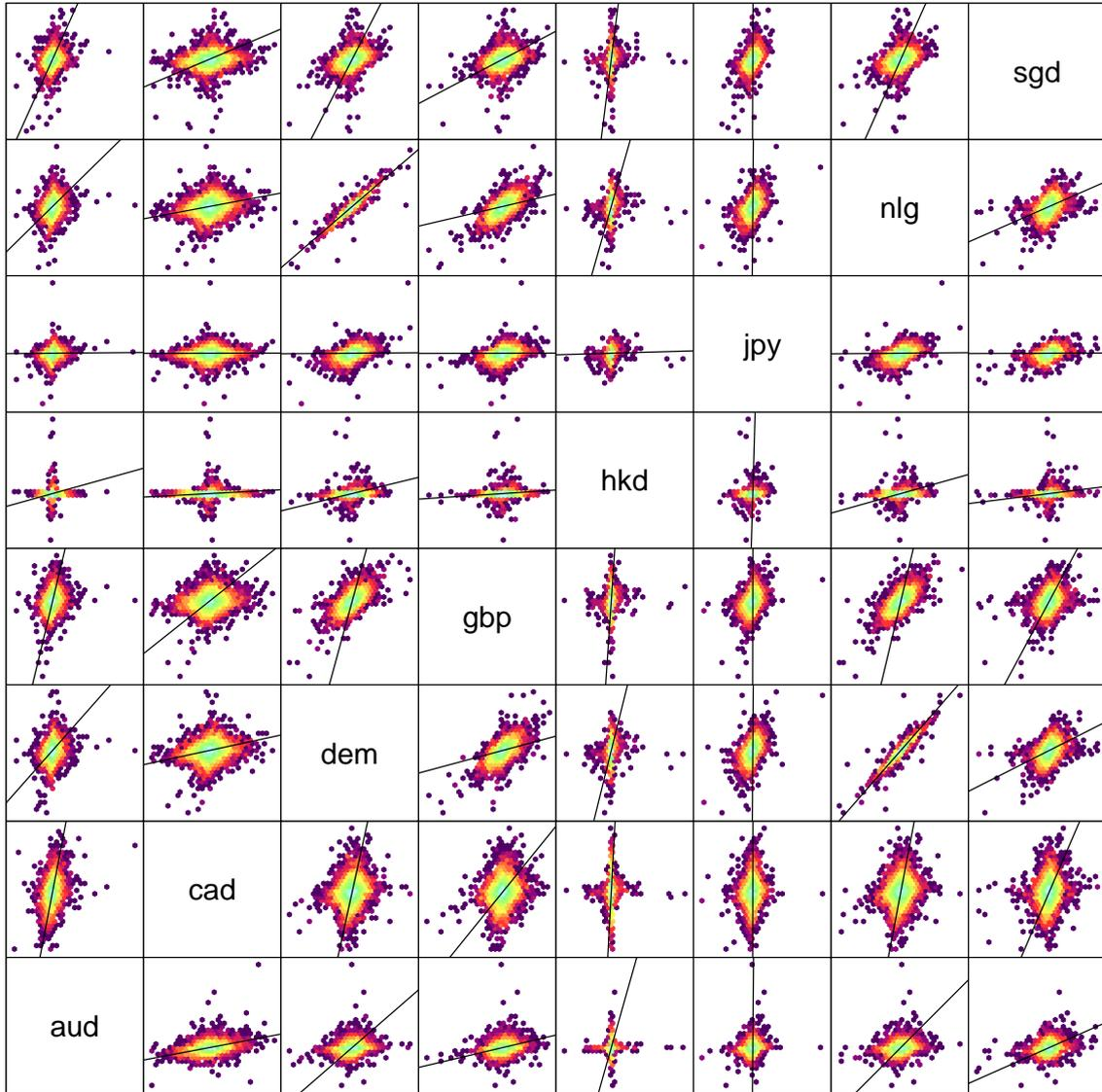


Figure 6: (top) $\bar{\alpha} - \lambda$ diagram for fit of empirical log returns of the WSI expressed in different currencies to SGH-distributions for time horizons from 5 min to 2.5 months (bottom) $\bar{\alpha} - \lambda$ diagram for fit of empirical log returns of major FX rates to SGH-distributions for time horizons from 5 min to 2.5 months



Scatter Plot Matrix

Figure 7: Color-encoded density plots of bivariate daily WSI log returns. The scale of the axes reaches from -0.11 to 0.11. The density is represented on a log scale. The colors are (ordered by increasing values) purple–red–orange–yellow–green.



Scatter Plot Matrix

Figure 8: Same as Fig. 7 for daily FX log returns. The scales of the axes are different for different plots. The relative scale of the x - and y -axes of an individual plot can be deduced from the inclination of the diagonal (continuous line).

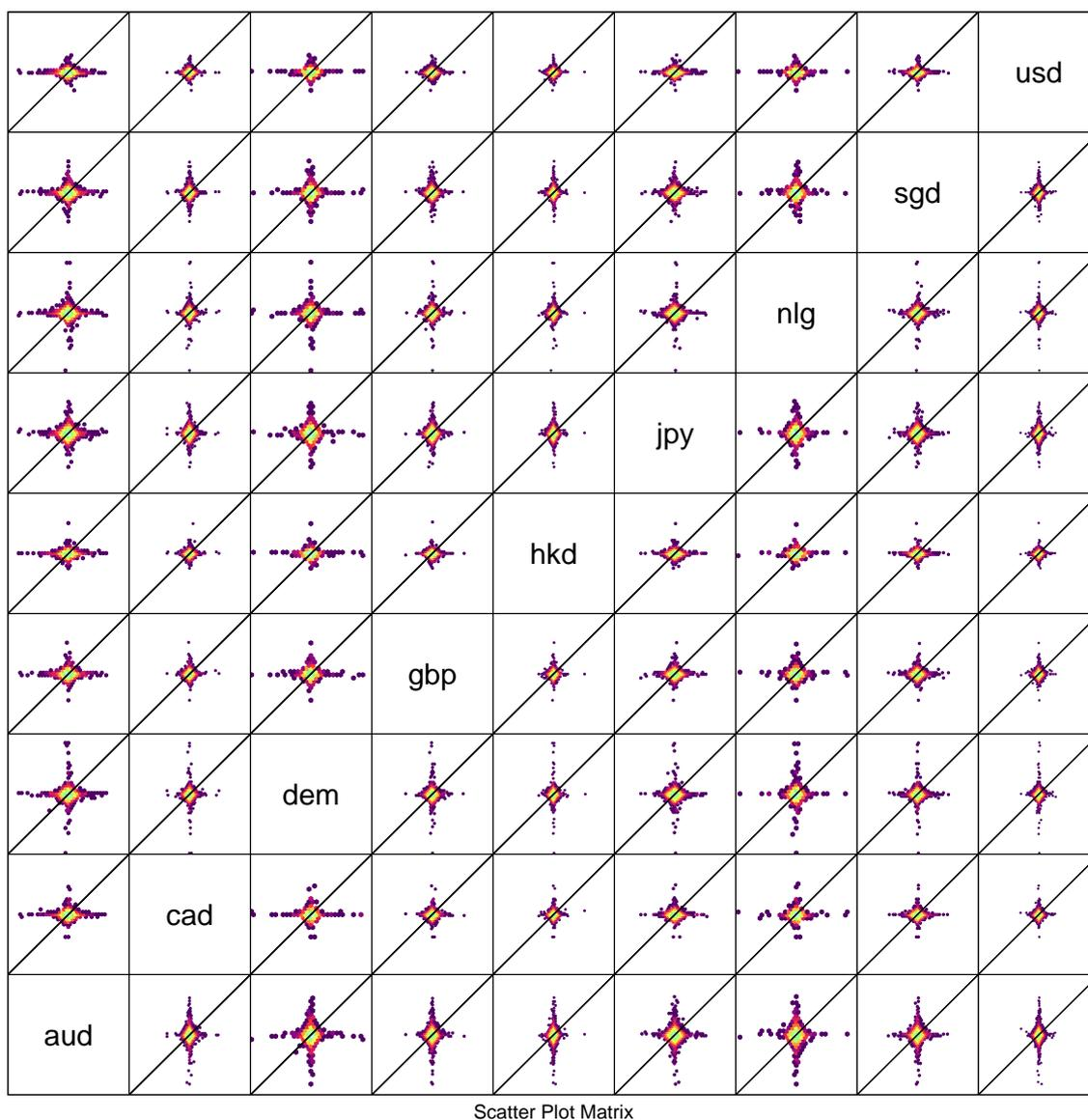
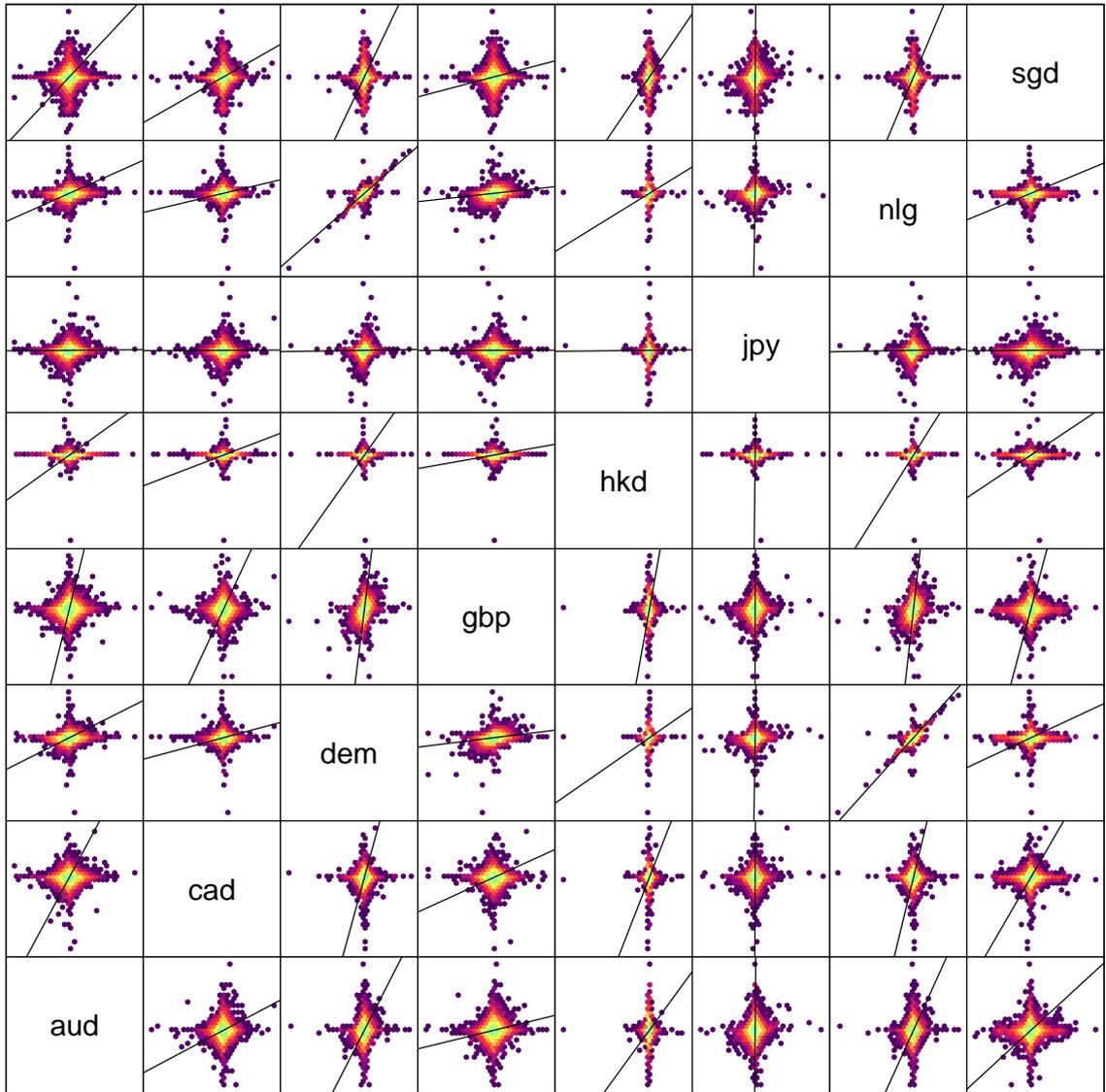


Figure 9: Same as Fig. 7 for 5 min WSI log returns. The scale of the axes reaches from -0.013 to 0.013.



Scatter Plot Matrix

Figure 10: Same as Fig. 8 for 5 min FX log returns.